XX IMEKO World Congress
Metrology for Green Growth
September 9–14, 2012, Busan, Republic of Korea

HIGH SPEED TEMPERATURE SENSORS IN EMISSION SYSTEMS OF COMBUSTION ENGINES

S. Augustin[1], F. Fröhlich[1], C. Ament[2], T. Güther[2]

[1] Institute for Process Measurement and Sensor Technology, Ilmenau University of Technology, Ilmenau, Germany,
[2] Department of System Analysis, Ilmenau University of Technology, Ilmenau, Germany,
silke.augustin@tu-ilmenau.de

Abstract: Temperature sensors used in emission systems of combustion engines must register enormous temperature differences within the shortest periods of time. This serves to protect the engine parts with respect to their temperature stability and to govern the energy efficient functioning of the engine. Numerical calculations according to the Finite Elements Method are used to estimate static-thermal measurement errors and dynamic characteristics primarily concerning medium specificity and construction of the temperature sensors. Prediction models are used to correct the dynamic behavior and to predict the medium temperature faster accurately.

Keywords: high-speed temperature sensor, numerical calculation, emission system, prediction.

1. INTRODUCTION

When using temperature sensors – especially contact thermometers – in technical processes, they have to be adjusted to the corresponding demands for the respective processes in industrial use. This concerns not only the demands for precise temperature measurement but also the prerequisites for use; according to various planned uses, the sensor has to endure extreme temperatures from -70 °C to 2,500 °C, chemical acids or extreme mechanical pressure. The sensor has to be maintenance free, stable, and functioning for years at a time. At the same time the demand remains to keep developing more exact temperature measurement and even faster sensors. This places even more extreme demands on the construction of the sensors, the selection of the materials used, and also on the evaluation electronics and data processing strategies.

Thermocouples used in exhaust systems of combustion engines are exposed to high temperature gradients and temperature leaps (ΔT > 900 K), high flow speeds and pressure. When constructing these thermocouples, a compromise is needed between the resulting high demands on the mechanical-thermal stability and the fast response time demanded by the automobile industry. Thermocouples have to be able to determine the temperature in the combustion cylinder within a few seconds. This exact temperature measurement serves to protect engine parts and is also important to optimally control the engine and fuel economy.

The study will show how numerical calculations from the Finite Elements Method can design the sensors in their construction and material selection in such a way that the above-mentioned demands are met. The first results of the calculations concerning the dependency of the static-thermal measurement error and the dynamic parameters of the construction and the boundary conditions are presented.

With the help of a special prediction model the dynamic errors as a function of the operating conditions can be corrected on-line.

2. NUMERICAL CALCULATIONS

The sensors have to measure the temperature exactly up to a maximal medium temperature of $T_M \approx$ 1,050 °C. The precision of the measured temperature is influenced by characteristic curve errors, errors in the evaluation electronics, by disturbance variables and thermal measuring errors.

The thermal measuring error is the temperature difference between the median sensor temperature $T_S(t)$ and the original medium temperature $T_M(t)$. This is subdivided into [1]:

Dynamic-thermal measuring error:

$$\Delta T_{th}(t) = T_S(t) - T_M(t) \tag{1}$$

Static-thermal measuring error:

$$\Delta T_{th} = T_S(t) - T_M \quad \text{for } t \to \infty \tag{2}$$

The static-thermal measuring error only occurs if heat transmission to a wall or surroundings happens, whose temperature differs from the medium temperature ($T_A \neq T_M$).

Typical parameters characterizing the dynamic performance of the sensors are time constants and time percent values. The dimension of the static-thermal measuring error and the time constants is determined by the effective thermal resistivity and by the heat transmission resistance as well as the heat capacities of the temperature sensor.

In order to optimize the static and dynamic behavior of temperature sensors, numerical calculations with the Finite Element Program ANSYS Workbench were conducted. The calculations are based on the solution of the Fourier Law of Heat Conduction [1, 2]:

$$c \cdot \rho \cdot \frac{\partial T}{\partial t} = \frac{\partial}{\partial x}\left(\lambda \cdot \frac{\partial T}{\partial x}\right) + \frac{\partial}{\partial y}\left(\lambda \cdot \frac{\partial T}{\partial y}\right) \frac{\partial}{\partial z}\left(\lambda \cdot \frac{\partial T}{\partial z}\right) + \dot{q}_e \qquad (3)$$

The values of density ρ, specific heat capacity c and the thermal conductivity λ depend from the temperature (for example: c of MgO-ceramic increase in the temperature range from 1060 to 1320 J/kg·K, λ decrease from 36 to 7 W/m·K [1]). This case was marked by extreme temperature gradients of 20…1,000 °C, which is the reason why temperature dependence of material data had to be taken into consideration for the numerical calculations.

The initial model for numerical calculations can be seen in figure 1. It shows the installation of the sensor into a turbocharger that has partially also been modeled in order to determine the parameter dependence of the location of installation and the Finite-Element-Mesh. The mesh includes more than 1.5 Mio. elements.

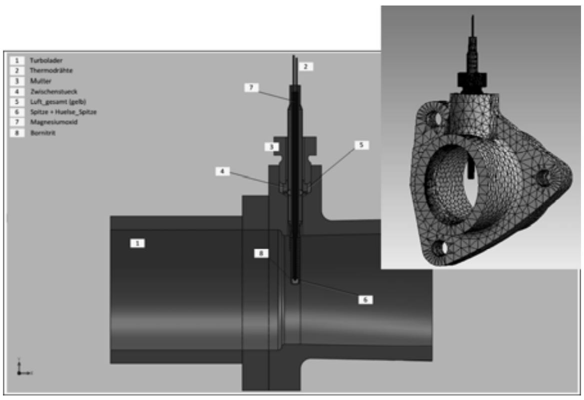

Fig. 1: FE model (sensor built into turbocharger)

To solve the differential equation of Fourier (3), the indication of specific boundary conditions is necessary, along with constructive and material parameters. According to the specific problem situation, this could be fixed temperature distributions, impressed heat flux or heat transmission from convection or radiation [2, 3]. The description of the boundary conditions is often problematic. There is no generally useful information in literature concerning the description of the boundary conditions in an engine compartment [4, 5] or in exhaust tracts. Numerical flow field calculations have been conducted, but their results have not yet proven to be experimentally verified in a turbocharger. In order to obtain initial experimental data, measurements of an engine test station were conducted using a specially prepared thermocouple element (figure 2).

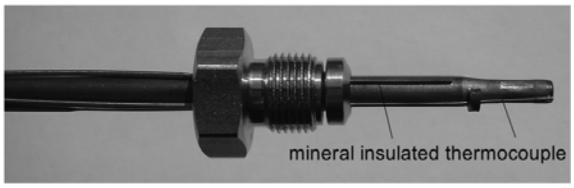

Fig. 2: Thermocouple with additional three mineral insulated thermocouples at the bottom, the middle and the screwing point

Fig. 3 gives examples of the measured temperatures after engine start, change of speed (t = 25 s) and after switch-off of the engine. As can be seen, at the time of t = 50 s there is a gradient of approx. 100 K in the engine compartment and of approx. 580 K towards the location of installation, both of which have to be borne in mind when setting the boundary conditions.

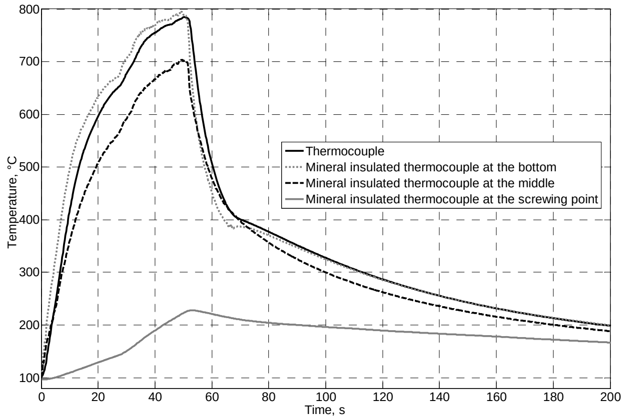

Fig. 3: Temperatures measured in the engine compartment with specialized thermocouple

The measured results show a temperature difference between the wall of the engine or turbocharger and the tip of the thermocouple.

Figure 4 demonstrates the calculated temperature fields with a constant heat-transfer coefficient of α = 1,000 W/m²K, heat transfer by radiation and a constant medium temperature of T_M = 980 °C in the location of installation. As for the surroundings, slightly moving air (heat-transfer coefficient of α = 30 W/m²K) with an ambient temperature of T_A = 25 °C was assumed.

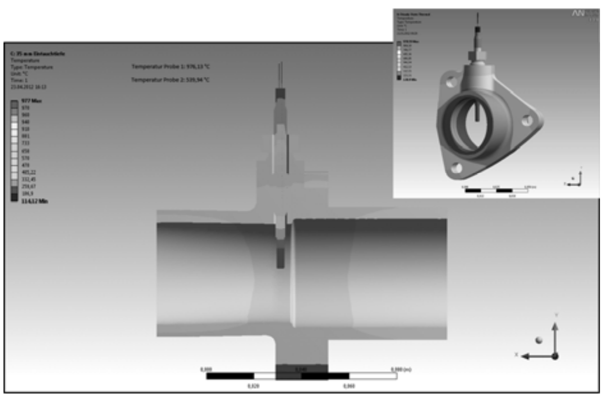
Fig. 4: Calculated temperature field in the turbocharger and sensor

Fig. 5 shows the calculated static-thermal measurement error by various heat transfer coefficients α. For this case, a maximum static-thermal measurement error of ΔT_{th} = 40.3 K by α = 200 W/m²K and a minimal static-thermal measurement error of ΔT_{th} = 0.01 K by α = 5,000 W/m²K was calculated.

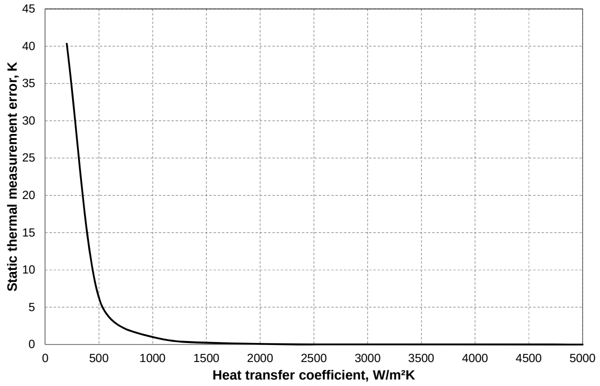

Fig. 5: Dependence of the static-thermal measurement error ΔT_{th} on the value of the heat transfer coefficient

It is assumed that the dynamic behavior concerning the temperature dependence of the material data differs in whether the temperature sensors are heated or cooled. In order to estimate how the dynamic behavior will change, calculations have been conducted with a constant heat-transfer coefficient α = 1,000 W/m²K. Temperature jumps were done from 100 °C to 1,000 °C up and down. Figure 6 demonstrates that the dynamic behavior slightly differs.

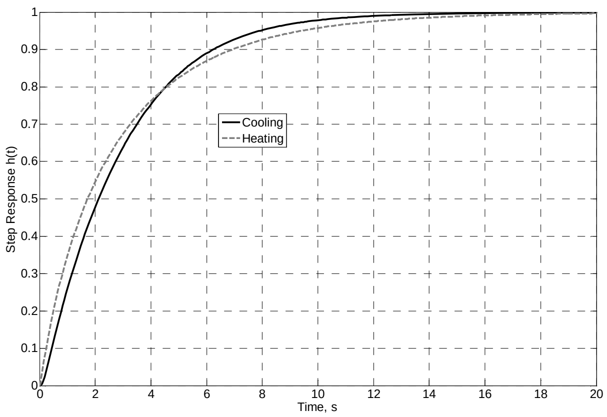

Fig. 6: Calculated step response when heating and cooling

3. MEASUREMENTS AND PREDICTION

Time percent values are determined normally by the step function response of a temperature sensor, which represents the temperature sequence of a sensor as a reaction to a sudden large change in the medium temperature. A better comparison of the step function responses of various sensor response flows is obtained in a standardized depiction. The characteristic time percent values t_{50}, t_{63} and t_{90} indicate when 50%, 63%, or 90% of the stationary final value is achieved [6].

The developed thermocouples were measured at turbocharger test equipment. The goal consisted of determining the dynamic behavior of the individual thermometers.

Therefore, a thermocouple with an outside diameter of 3.2 mm and a reference thermocouple with an outside diameter of 2.0 mm were analyzed. With the latter sensor, that cannot be part of the normal operation in a vehicle due to its lack of mechanical-thermal stability, the medium temperature was to be measured fast in order to collect more accurate data on the real course and dimension of the medium temperature.

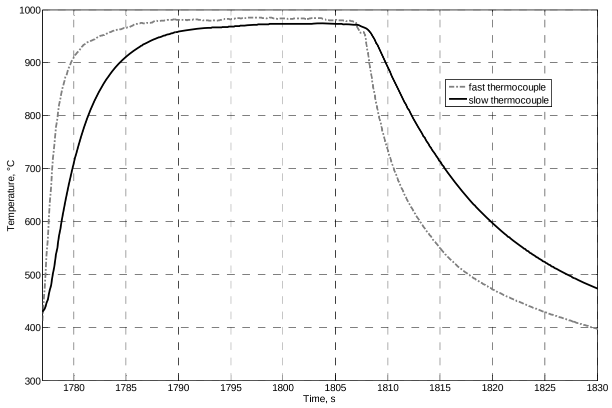

Fig. 7: Measurement at turbocharger with different thermocouples

From the measured step responses by heating, the time percent values and the time constants were determined.

Table 1: Measured time percent values and the calculated time constant

	t_{50} / s	t_{63} / s	t_{90} / s	T_1 / s
slow thermocouple	2.95	3.95	8.63	3.53
fast thermocouple	0.98	1.3	3.62	1.64

A possible description method of the transfer characteristics is found in the time constants of the system. The combination of time constants with the respective transfer element enables the model description of every real system.

The approach presented here starts with a determination of the specific time constants as well as the sensor system's transfer elements in the model. The second step is the prediction, which comprises an estimation concerning the current temperature, taking into account the sensor's measurement results. The realized measurements show that the temperature sensors in use with a lag element of the first order (PT1 transfer element) and thus only one time constant can be described sufficiently (fig. 8). It consists of a proportional component K and a lag component T1[7].

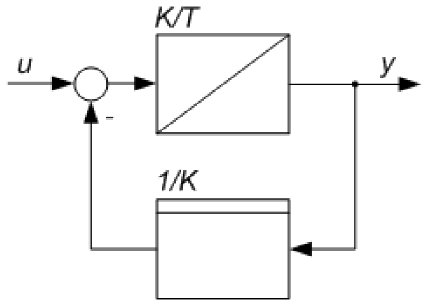

Fig. 8: Structure of PT1 element

$$T_1 \cdot \dot{y}(t) + y(t) = K \cdot u(t) \qquad (4)$$

For the identification of the absolute terms of K and T, we compared the measured temperature data with the ambient temperature data in the Matlab 'ident' Toolbox [8], $u(t)$ being the thermal excitation in °C and $y(t)$ the temperature measured by the thermocouple also in °C. The time constant T1 is determined by the material characteristics and the geometry of the sensor and is identified experimentally (or numerically), as shown above.

This model is transferred into a state space representation, since the Kalman filter is based on this representation. The model of the first order is described in the state space by the matrices [7].

$$A = \left[-\frac{1}{T_1}\right], \; B = \left[\frac{K}{T_1}\right] \text{ und } C = [1] \qquad (5)$$

The state space differential equation and the initial equation are:

$$\dot{x}(t) = \left[-\frac{1}{T_1}\right] \cdot x(t) + \left[\frac{K}{T_1}\right] \cdot u(t), \quad y(t) = [1] \cdot x(t) \qquad (6)$$

Transformation of the input into an estimated state

A filter that compensates the lagging sensor dynamics is to be realized, estimating the unknown thermal excitation that forms the input $u(t)$ of the above mentioned system. In order to have a suitable model for this task, the previous input is integrated into the state vector:

$$x_{neu}(t) = \begin{bmatrix} x(t) \\ u(t) \end{bmatrix} \qquad (7)$$

As a result, the system and output matrix is extended while the input matrix is broken down, leaving the new system autonomous:

$$A_{neu} = \begin{bmatrix} A & B \\ 0 & 0 \end{bmatrix}, \qquad B_{neu} = 0, \; C_{neu} = [C \quad 0] \qquad (8)$$

For the thermal system,

$$A_{neu} = \begin{bmatrix} -1/T_1 & K/T_1 \\ 0 & 0 \end{bmatrix}, \qquad B_{neu} = 0, \; C_{neu} = [1 \quad 0] \qquad (9)$$

applies.

The observability of the new system is a prerequisite for the successful filter layout. Following the Kalman criterion [9], the observability matrix must be of full order:

$$Q_B = \begin{bmatrix} C \\ CA \end{bmatrix} = \begin{bmatrix} 1 & 0 \\ -1/T_1 & K/T_1 \end{bmatrix}, \quad \det Q_B = K/T_1 \qquad (10)$$

This is fulfilled for T1>0.

Time discretization of the model

In relation to a future embedded realization of the filter, a time-discrete implementation is more efficient than a time-continuous one. This requires the transformation of the continuous model into a discrete one. With the sampling rate time T, the discrete system matrix now is:

$$F = e^{(A_{neu} \cdot T)}, \qquad (11)$$

while the output matrix remains unchanged.

Algorithm of the time-discrete Kalman filter

In order to predict an estimated value at a specific time (k+1) with the values measured by a sensor until a specific time (k), a discrete Kalman filter is used [8], applying an a priori estimate of the measured value for the time (k+1) in the first phase of prediction. The parameters of this estimation are adapted in the correction phase according to the then measured value at a time (k+1).

Both steps, which are repeated cyclically for every time step, consist of five equations:

Discrete Kalman filter: time update equations:

$$\begin{aligned} \hat{x}_{\bar{k}} &= F \cdot \hat{x}_{k-1} + B \cdot u_{k-1} \\ P_{\bar{k}} &= F \cdot P_{k-1} \cdot F^T + Q \end{aligned} \qquad (12)$$

Discrete Kalman filter: measured value update equations

$$\begin{aligned} K_k &= P_{\bar{k}} \cdot H^T \cdot \left(H \cdot P_{\bar{k}} \cdot H^T + R\right)^{-1} \\ \hat{x}_k &= \hat{x}_{\bar{k}} + K_k \cdot \left(y_k - H \cdot \hat{x}_{\bar{k}}\right) \\ P_k &= \left(I - K_k \cdot H\right) \cdot P_{\bar{k}} \end{aligned} \qquad (13)$$

In these equations, Q represents the covariance matrix of the process noise and R the covariance matrix of the measurement noise. In the recursion equations, not only the state x is updated, but also the covariance matrix of the measurement error P, it can thus be used as a measure for the estimation's quality.

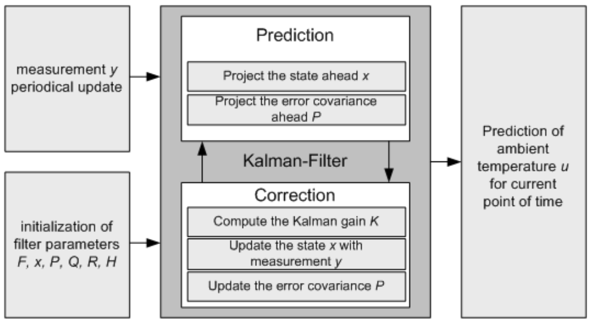

Fig. 9: Structure of the Kalman filter

This modified Kalman filter was implemented in Matlab Simulink [10].

Results of the signal estimation

The filter algorithm allows the desired estimation of the original system input value (temperature) with the help of the measured values by the temperature sensor.

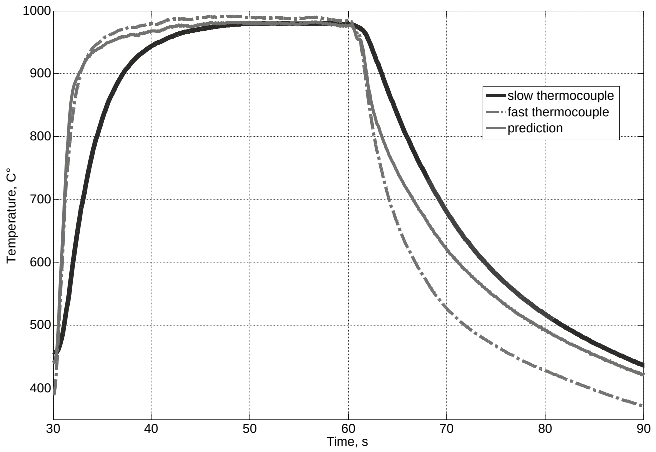

Fig. 10: Measurement and result of prediction at turbocharger

The aim, which is to estimate thermal excitation (sensor signal of the fast thermocouple) from the input values of the slow sensor, was fulfilled with the prediction model used in this study (fig. 10). By using the Kalman filter, the actual ambient temperature can be estimated with significantly decreased time-delay. Through this, it is possible to control processes with high dynamics in real-time.

4. CONCLUSIONS

The numerical and experimental analyses prove that the developed temperature sensors fulfill the requirements concerning dynamic parameters for the tested sensor designs. Nevertheless, further numerical calculations have to be conducted regarding the minimization of static-thermal measurement errors.

With the prediction, the dynamic and static errors of the temperature sensors can be corrected during the measurement.

Research was conducted within the scope of the projects "High Speed Multisensorics" (BMWi, reference number KF2007412JT0) and "MESA – Methodic development of energy-efficiency-raising and pollutant-minimizing emission systems and their components" (ThIMO, TMWAT, ESF, reference number 2011 FGR 0112). The authors would like to say thank you for the financial and organizational support. We would also like to thank the colleagues of the involved companies as well as the colleagues of the Departments of Automotive Engineering at TU Ilmenau.

5. REFERENCES

[1] Grigoriev, I. S., Meilikhov, E. Z.: "Handbook of physical quantities"; CRC Press, 1997

[2] Bernhard, F. (Herausgeber): Technische Temperatur-messung; Springer-Verlag, 2004.

[3] Groth, C., Müller, G.: „FEM für Praktiker – Band 3: Temperaturfelder"; expert Verlag, 1995

[4] Woschni, G., Kolesa, K., Spindler, W.: „Isolierung der Brennraumwände – Ein lohnendes Ziel bei Verbrennungsmotoren?"; in MTZ Motortechnische Zeitschrift 47, 1986

[5] Bargende, M.: „Ein Gleichungsansatz zur Berechnung der instationären Wandwärmeverluste im Hochdruckteil von Ottomotoren"; Dissertation, TH Darmstadt, 1991

[6] Augustin, S., Fröhlich, T., Mammen, H., Irrgang, K. Meiselbach, U.: Determination of the dynamic behaviour of high-speed temperature sensors; Measurement Science and Technology; 2012

[7] Föllinger, O.; Dörrscheidt, F.; Klittich, M.: „Regelungstechnik, Einführung in die Methoden und ihre Anwendung", 8. überarbeitete Auflage, Hüthig GmbH Heidelberg

[8] The MathWorks, "System Identification Toolbox - Documentation", 2011, Available: http://www.mathworks.com/help/toolbox/ident/, accessed 2012-01-12.

[9] Kalman, R.E., 1960, A New Approach to Linear Filtering and Prediction Problems.

[10] The MathWorks, "Simulink - Simulation und Model-Based Design", 2011, Available: http://www.mathworks.de/products/simulink/index.html, accessed 2012-01-19.